

# Hydraulic Characteristics and Sediment Yielding on Engineering Excavated Soil Slope under Simulated Rainfall

Xi Li, Chongqing Wang, Shixiong Jiang, Sunxian Weng, Yanhong Che, and Yao Chen\*  
*Electric Power Research Institute of State Grid Fujian Electric Power Co., Ltd., Fuzhou 350007, P. R. China*

**Keywords:** Engineering excavated slope, Simulated rainfall, Hydrodynamics, Inter rill erosion, Model

**Abstract:** Engineering excavated soil slopes play an important role in artificial soil loss. In order to assess the impact of these engineering excavated soil slopes, hydraulic characteristics and sediment generation must be quantified. Field rainfall simulation experiments were conducted under five rainfall intensities (0.6, 1.1, 1.61, 2.12 and 2.54 mm/min) and three slope gradients (10°, 15° and 20°) on engineering excavated soil slopes. The precipitation of each rainfall was set to 50 mm, the duration of rainfall was 83, 45, 31, 24 and 20 min for simulated rainfall intensities of 0.6, 1.1, 1.61, 2.12 and 2.54 mm/min respectively. Plots used in this study were laid out to be 3 m in length and 1 m in width. Calibration of rainfall intensities was conducted before each experiment. Totally, 45 simulated rainfall events were performed. Three indices were used to research the soil erosion processes, including surface and subsurface runoff volume and the sediment yield. Results showed that: 1) both surface and subsurface runoff varied depending on slope gradient and rainfall intensity. Surface runoff and subsurface runoff were 33.6~42.7 mm and 0.15~1.24 mm, respectively. The process of surface runoff yield was the main hydrological process, accounting for 67.2~85.4% of the precipitation. Under conditions of low (0.6 mm/min) and high (2.12 and 2.54 mm/min) rainfall intensity, surface runoff increased with slope. 2) The averaged flow velocity, Reynold number, Froude number, Darcy-Weisbach friction coefficient, Manning roughness coefficients and stream power were 0.047~0.104 m/s, 48.985~392.918, 0.355~0.581, 1.317~5.171, 0.044~0.101 m<sup>-1/3</sup>.s, 0.029~0.457 kg·s<sup>-3</sup>, respectively. In addition, flow velocity and Reynold number had a greatly significant correlation with rainfall intensities, Manning roughness coefficients, Darcy-Weisbach friction coefficients and stream power a weak correlation with rainfall intensity, Froude number had a weak correlation with rainfall and slope. There was no obvious relationship between Darcy-Weisbach friction coefficient and the Reynolds number and there was a “increase resistance” phenomenon in engineering excavated soil slopes. 3) Interrill erosion was the main erosion form on engineering excavated soil slopes. Rainfall intensity, runoff rate and slope gradient are key factors to model sediment yield rate. Three commonly interrill erosion models were evaluated and compared, the fitness of model followed the pattern: model 1(NSE=0.977)>model 2(NSE=0.966)>model 3(NSE=0.924). A further comparison between the models showed that the convex curvilinear slope factor (model 1) was more precise than the power (model 2) and linear (model 3) slope factor in describing the effect of slope gradient for this data. Interrill erodibility adopted in the WEPP model was determined as 0.332×10<sup>6</sup> kg·s·m<sup>-4</sup>. The results provide valuable data for establishing water erosion prediction model of engineering excavated slope.

## 1 INTRODUCTION

Erosive rainfall is one of the main driving factors of slope hydraulic erosion. Rainfall indicators such as rainfall volume, rainfall intensity and rainfall ephemeris jointly influence the slope erosion process. Pruski and Nearing (2002) found that soil loss increased by 0.85% when the total rainfall increased by 1% for the same rain intensity conditions. The raindrop striking splash not only causes separation

and displacement of soil particles, but also increases the turbulence of water flow in the thin layer of the slope. The boundary conditions of water flow in indoor soil tank test are easy to control. It is a more common method to study soil erosion dynamics of slope, but it has large differences with natural slope. As one of the most widely distributed and hazardous sources of anthropogenic soil erosion, soil excavation slopes are mainly excavated after topsoil stripping for construction projects. The disturbed soil is generally composed of weathered crust or parent material

(parent rock) (Zhang et al., 2013). Soil excavation slopes have high soil capacity, high compactness, and steep slope, thus resulting in a soil loss process that differs significantly from that of natural slopes. Under the erosive rainfall, the water flow along the excavated slope of the project constantly has the convergence of mass sources, and the temporal and spatial changes of runoff are obvious, and the soil porosity of the lower bedding surface is lower, and the infiltration capacity is poorer than that of the natural slope surface, which is more complicated.

At present, there are relatively few studies on the erosion characteristics of engineering excavation surfaces and their erosion mechanisms. Most studies have focused on the erosion of loose piles generated by mineral extraction and road construction. For the prediction model of soil erosion on excavated slopes, the current research is still in the initial stage. Therefore, this study analyzes the hydrodynamic characteristics of erosion between fine trenches on soil excavation slopes and its loss prediction under erosive rainfall conditions by field artificial rainfall test method, with a view to providing a theoretical basis for the prediction and control of anthropogenic soil erosion caused by engineering construction excavation.

## 2 MATERIALS AND METHODS

### 2.1 Experimental Design and Observation

Three slope plots of 3 m in length and 1 m in width were selected for this experiment on a highway slope in central China, with the slopes of 10°, 15° and 20°. The wall of the slot is made of stainless steel plate of 2 mm thickness to cut off the channel of runoff exchange inside and outside the cell. A "V" shaped catch basin was inserted at the lower end of the plot and connected to a runoff collection barrel through the catch basin to collect surface runoff, the structure of which is shown in Figure 1.

The test uses a spray-swing simulated rainfall device. The rainfall height was 2.5 m, the rainfall uniformity was 85%, the effective rainfall area was about 2 m×3 m, the simulated rain intensity range was 20~170 mm/h, and the simulated rainfall approximated natural rainfall. In view of the range of erosive rainfall occurring at the test site, the rainfall intensities of 0.6, 1.1, 1.61, 2.12 and 2.54 mm/min were finally designed for the combined tests. The total amount of rainfall for each rainfall test was controlled at 50 mm, and the rainfall ephemeris was set according to the rainfall intensity, i.e., the rainfall intensities for 83, 45, 31, 24 and 20 min were 0.6, 1.1, 1.61, 2.12 and 2.54 mm/min, respectively.

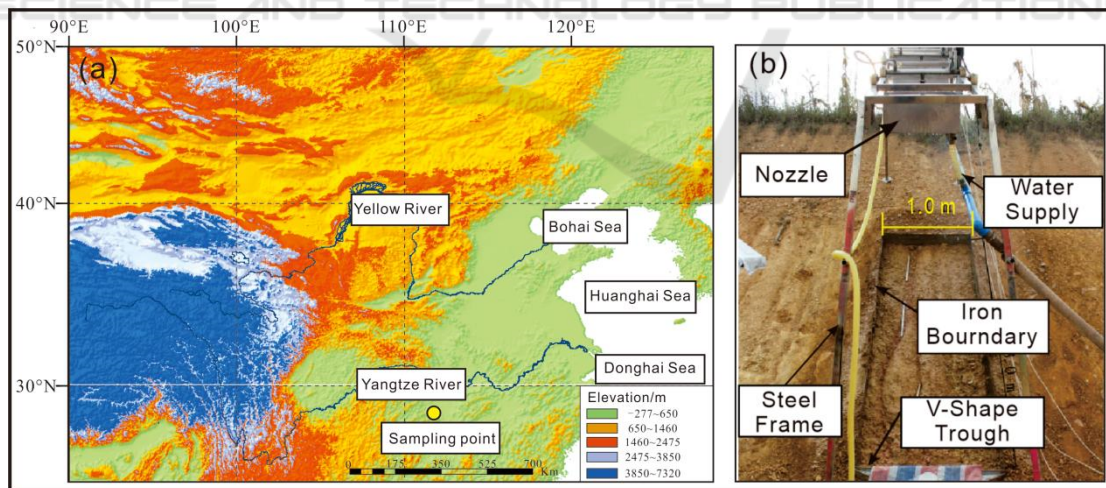


Figure 1: (a) Sampling point location;(b) Diagram of runoff and sediment collection system in the field.

The soil capacity of the road excavation slope of the test site was measured by the ring knife method to determine 1.54~1.58 g/cm<sup>3</sup>. The average capacity of the test plot was 1.56±0.21 g/cm<sup>3</sup> and the average water content was 17.6±0.18%. The slope of the

excavated surface is between 10° and 70°, with 40° to 70° accounting for 19%, 20° to 40° accounting for 75% and 20° accounting for 6%. Through particle sieving of the collected soil samples, it was found that the soil on the excavated slope was dominated by 1~2

mm soil particles with coarse texture, and the basic soil properties are shown in Table 1.

Table 1: Physical-chemical properties of the test soil.

Soils	Particle composition/%	
	Particle size/ mm	Mass percent/%
Disturbed soil	<0.01	0.19
	0.01~0.1	4.48
	0.1~0.5	22.10
	0.5~1	21.68
	>1~2	51.56

## 2.2 Test Process

A rain shelter was used to cover the plot before the start of each test. Rain barrels were placed around the perimeter of the plot to filter the rain intensity until the rainfall intensity reached the test requirements. Soil samples were collected on the excavated surface to determine the pre-soil water content. When the soil moisture content of the repeated tests showed a large difference, it was left to stand for 24 hours after a light rainfall in advance to eliminate the effect of soil moisture content. From the beginning of the experiment to the full production of flow on the slope, the flow rate and sand content at the outlet were measured and the time was recorded. During the test, the water flow temperature is used to calculate the water flow viscosity coefficient, while the total time of rainfall is also recorded. Further, the sampling interval was determined as one sample every 1 minute at the beginning of the birth flow. After 3-7 minutes, a sample was taken every 2 minutes. After 7-10 minutes, one sample was taken every 3 minutes. After 10 minutes, a sample was taken every 5 minutes. The sediment content in the sample is determined by drying method. The surface flow velocity was determined by  $KMnO_4$  pigment tracer method in three measurement sections at the top, middle and bottom, and each test was repeated three times to ensure the test accuracy. After the test, the new plot was rearranged for the test.

## 2.3 Data Analysis Method

1) Surface runoff velocity ( $V$ ). The maximum surface flow velocity was measured at three observation sections using  $KMnO_4$  solution and an electronic stopwatch to determine the time required to pass the 1 m measurement distance, and the average value was taken and multiplied by a correction factor of 0.67 to

obtain the average surface runoff flow velocity (Li et al., 2015),  $m \cdot s^{-1}$ .

2) Average water depth ( $H$ ). Since the erosion of the soil excavation slope during the test was dominated by the erosion between fine trenches and the water depth was small, it was difficult to determine directly. Therefore, equation (1) was used for calculation (Wang et al., 2016):

$$h = \frac{Q}{V \cdot B \cdot t} \quad (1)$$

Where,  $h$  is the average water depth on the slope,  $m$ ;  $Q$  is surface runoff flow,  $m^3$ ;  $B$  is the cross-section width,  $m$ ;  $t$  is the time,  $s$ .

3) Calculation of hydrodynamic parameters. The hydrodynamic parameters involved in this paper include Reynolds number  $Re$ , Darcy-weisbach drag coefficient  $f$ , Manning's roughness coefficient  $n$  and flow power  $w$ . The above parameters were calculated using the open channel flow equation (Luo et al., 2009).

4) Soil denudation rate ( $D_i$ ) is the mass of soil transported by surface runoff per unit area per unit time,  $kg \cdot (s^{-1}m^{-2})$ , which is calculated as follows:

$$D_i = \frac{M_s}{A \cdot t} \quad (2)$$

Where,  $M_s$  is the soil loss from the slope in the time period  $t(s)$ ,  $kg$ , obtained from runoff sediment samples.  $A$  is the area of the test plot,  $m^2$ .

5) In this paper, three commonly used statistical models of inter-groove erosion on slope surfaces are used to study their applicability in predicting inter-groove erosion on soil excavation surfaces.

Model 1 adopts WEPP inter rill erosion equation (Flanagan & Nearing, 1995):

$$D_i = K_i Q S_f I \quad (3)$$

In which,  $K_i$  is the erodibility factor between rills,  $kg \cdot s \cdot m^{-4}$ ;  $Q$  is the average runoff intensity,  $m \cdot s^{-1}$ ;  $S_f$  is the slope factor and the slope of the test plot;  $I$  is rain intensity,  $m \cdot s^{-1}$ .

Model 2 adopts the inter rill erosion equation including runoff factor proposed by Kinnell (1993):

$$D_i = K_i Q S I \quad (4)$$

Where,  $Q$  is the average runoff intensity,  $m \cdot s^{-1}$ ;  $S$  is the slope of the test area,  $m \cdot m^{-1}$ .

Model 3 adopts the inter rill erosion equation proposed by Bulygin et al. (2002):

$$(5)$$

SPSS 20.0 was used for data analysis, and LSD (lowest extreme difference method) was applied in ANOVA for multiple comparisons with a significance level of  $p < 0.05$ . The model accuracy evaluation metrics were selected from the complex correlation

coefficient ( $R^2$ ) and the Nash-Sutcliffe efficiency coefficient (NSE), where the NSE was calculated using the following equation (Bulygin et al., 2002):

$$(6)$$

Where  $O_i$  is the measured value,  $O_c$  is the calculated value and  $O_m$  is the average value of the measured value.

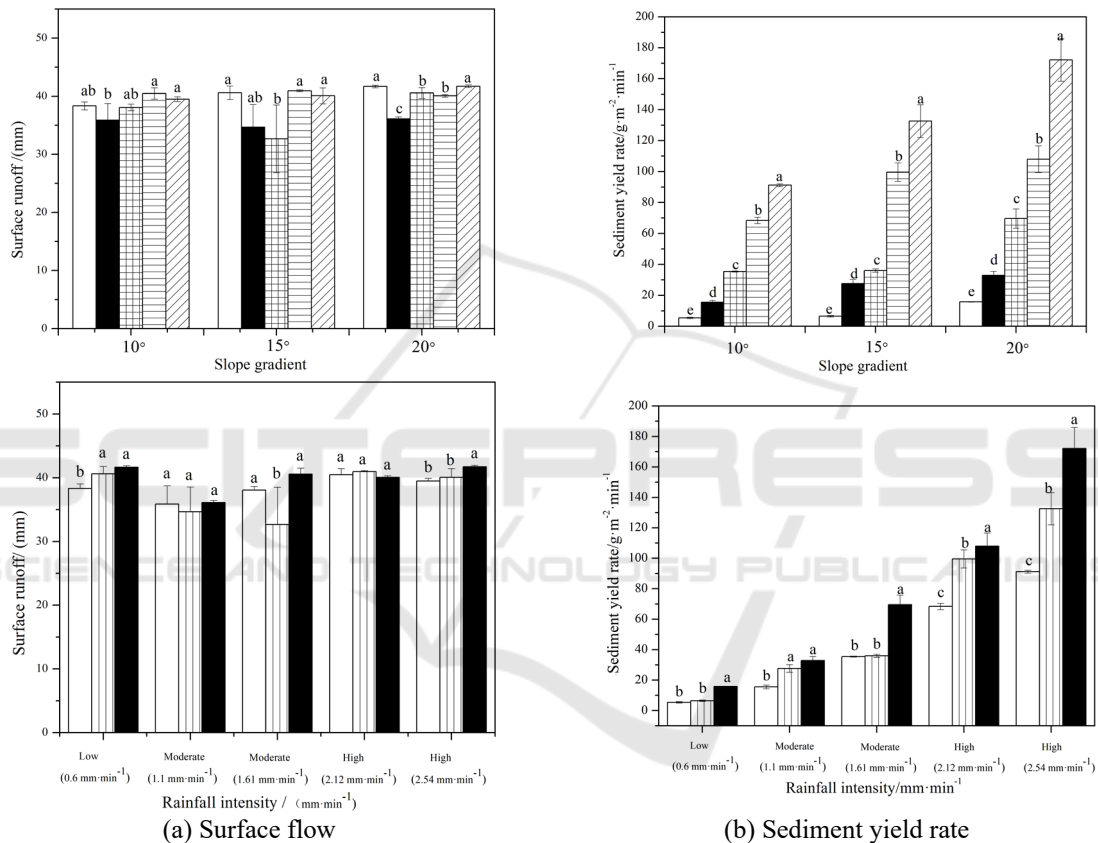


Figure 2: Surface runoff volume and sediment yield rate for different slope gradients and rainfall intensities. For each treatment, means with the same lower-case letter are not significantly ( $p < 0.05$ , least significant difference) different.

### 3 RESULTS AND ANALYSIS

#### 3.1 Analysis on Characteristics of Water and Soil Loss on Soil Excavation Slope

Surface runoff from soil excavation slopes varied between 33.6 and 42.7 mm under different slope and rain intensity conditions (Figure 2a). Surface runoff, as the main hydrological process under erosion

conditions, accounted for 67.2 to 85.4% of the total rainfall. A study by Defersha and Melesse (2012) indicated that the effect of slope and rain intensity on sand and flow production on slopes varies with changes in soil properties on the subsurface. In this study, an artificially simulated rainfall scheme was adopted to control the total rainfall of 50 mm with rainfall intensities of 0.6, 1.1, 1.61, 2.12 and 2.54 mm/min. Under the same slope condition, the surface runoff volume shows a phenomenon of decreasing and then increasing with the increase of rain intensity,

which is due to the fact that when the soil on the slope surface produces crust, it will make the slope surface flow production mechanism become more complicated. When the rain intensity changes from small to medium rain intensity, the splash of raindrops is further enhanced. The soil compacted by the excavation is further transported and the soil porosity increases, thus increasing the soil infiltration. With the further increase of rainfall intensity, the rainfall intensity is greater than the infiltration rate, forming superinfiltration production flow and accelerating the formation of surface runoff. The increase of surface runoff flow rate will reduce the chance of infiltration of slope surface flow. Therefore, the surface runoff appears to decrease and then increase with the increase of rainfall intensity.

There were significant differences in sand yield per unit area under different slope and rain intensity conditions (Figure 2b), and the sand yield per unit area increased with the increase of slope and rain intensity. When the slope of excavation slope increases from 10° to 20°, the sand production rate per unit area increases by 2.92, 2.12, 1.96, 1.57 and 1.88 times when the rain intensity is 0.6 mm·min<sup>-1</sup>, 1.1, 1.61 mm·min<sup>-1</sup>, 2.12 and 2.54 mm·min<sup>-1</sup>, respectively. On the other hand, the sand production rate per unit area increased 16.87, 20.48 and 10.88 times when the rainfall intensity increased from 0.6 mm min<sup>-1</sup> to 2.54 mm min<sup>-1</sup> at slopes of 10°, 15° and 20°, respectively. This is consistent with the findings of Ziadat and

Taimeh (2013). The effect of variation in rainfall intensity on sand production rate is greater than the effect of slope variation on sand production rate.

### 3.2 Analysis on Hydrodynamic Parameters of Soil Excavation Slope

Table 2 shows the correlation coefficient statistics of hydrodynamic parameters with slope S, rain intensity I and rain intensity-slope interaction (I×S). Under different rain intensity conditions, the surface runoff velocities V of 10°~20° soil excavation slopes were 0.047~0.084, 0.052~0.092 and 0.054~0.104 m·s<sup>-1</sup>, respectively. The flow velocity V increased with increasing rain intensity at the same slope. There is a significant linear relationship between the two (R<sup>2</sup>=0.58-0.92, P<0.01). Under the same rainfall intensity, the runoff flow velocities of slopes of 15° and 20° were 0.84-1.19 times and 0.92-1.23 times higher than those of slopes of 10°, respectively. The differences between the runoff velocities of excavated slopes with different slopes of soil were not significant (P>0.05). The results of correlation analysis showed that the soil excavation slope flow velocity was not significantly correlated with slope (P>0.05) and was highly significantly correlated with rain intensity I and the interaction of slope and rain intensity I×S (P<0.01).

Table 2: Correlations between flow hydrodynamic parameters and coupling effects of rainfall intensity and slope gradient.

Variable	$V/(m \cdot s^{-1})$	$Re$	$Fr$	$f$	$n/(m^{-1/3} \cdot s)$	$w/(kg \cdot s^{-3})$
$I$	0.892**	0.954**	-0.199	0.091	0.397	0.759
$S$	0.198	0.213	-0.052	/	/	/
$I \times S$	0.878**	0.918**	-0.109	/	/	/

The Reynolds number of soil excavation slope runoff under different rain intensity and slope conditions is between 48.985 and 392.918, and the soil excavation slope runoff flow pattern belongs to the category of laminar flow according to the criteria for determining the flow pattern of open channel flow. In the test, it was observed that no matter what the combination of rain intensity and slope, there was obvious sand-holding phenomenon in the process of slope flow movement. The sand concentration of the water body at the outlet of surface runoff is between 1.2% and 23.7%. The slope runoff flow pattern should belong to the category of turbulent flow. The traditional criteria for determining the flow pattern of open channel flow are not applicable to the soil excavation slope. Re had the highest correlation with

rainfall intensity I and insignificant correlation (P>0.05) with slope S (Table 2), indicating that the magnitude of rainfall intensity determines the variation of runoff patterns on the soil excavation slopes. The Froude number Fr is between 0.355 and 0.581, all of which are less than 1 and are slow flow. Correlation analysis showed that the correlation between Fr and the interaction of rain intensity I, slope S and rain intensity I × S was not significant (P>0.05).

The Darcy-Weisbach resistance coefficient f and the Manning coefficient n are hydraulic parameters commonly used to characterize the resistance to water flow on a slope. Under different rain intensity conditions, the runoff resistance coefficient of excavation slope at slope of 10° ranged from 1.317 to

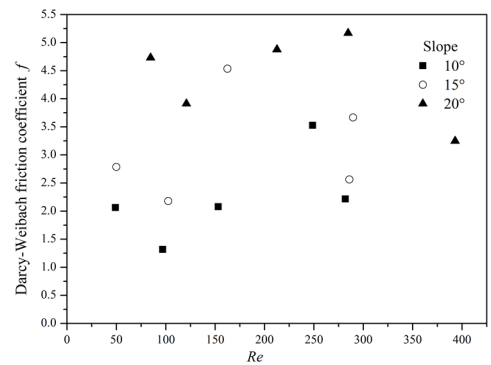
3.527. Under the same rain intensity conditions, the  $f$ -values of  $15^\circ$  and  $20^\circ$  soil excavation slopes are 1.04-2.18 times and 1.46-2.97 times higher than those of  $10^\circ$  slopes. The  $f$ -value of soil excavation slope increases with the increase of slope. At the same slope, there is no significant trend in the  $f$ -value of soil excavation slope with rain intensity. The Manning coefficients  $n$  of  $10^\circ$ ~ $20^\circ$  soil excavation slope is 0.044~0.084, 0.057~0.090 and 0.079~0.101 respectively. The correlation between the  $f$  and  $n$  values of the soil excavation slope and the rain intensity was not significant. A power function relationship exists between the slope flow resistance coefficient  $f$  and the Reynolds number  $Re$  (Nearing et al., 1997). The results of this test show that there is no significant relationship between  $f$  and  $Re$  (see Figure 3a). The Reynolds number is not the main factor affecting the resistance coefficient because the particle resistance of the soil excavation slope does not dominate. This is in agreement with the findings of Nearing et al. (1997). On rough slopes, there is no single relationship between  $f$  and  $Re$  As can be seen from Figure 3b, the resistance of slope flow under rainfall conditions is greater than that under non-rainfall conditions, and the extent of its effect is influenced by the depth of water flow, slope and surface morphology. There is an obvious phenomenon of "increasing resistance" of water flow on the slope of soil excavation.

The water flow power  $w$  incorporates the role of slope and runoff rate. Soil flow can be predicted in terms of water flow dynamics. The water flow power ranged from 0.029 to 0.457  $\text{kg}\cdot\text{s}^{-3}$  for different slope and rain intensity conditions. Under the same conditions of rain intensity, the water flow power ( $w$ ) of slope  $15^\circ$  and  $20^\circ$  is 1.517~1.745 times and 2.282~3.379 times than that of slope  $10^\circ$ . The  $w$  value increases as the slope increases. The correlation between  $w$  value and rain intensity is not significant. The relationship between the power of water flow and the amount of soil loss per unit was obtained from the regression analysis, as follows:

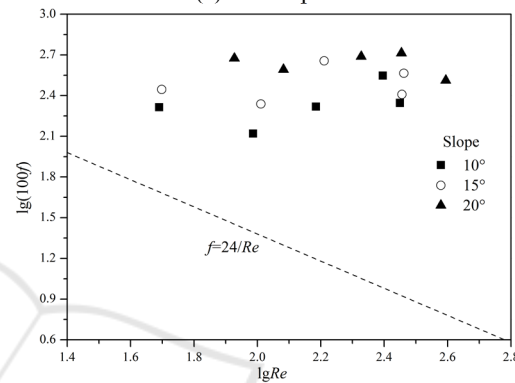
(7)

Where,  $qs$  is the unit soil loss,  $\text{g}\cdot\text{s}^{-1}\cdot\text{m}^{-1}$ ;  $W$  is the water flow power,  $\text{g}\cdot\text{s}^{-3}$ .

From equation (7), it can be seen that the linear relationship between water flow power and unit soil loss has a high coefficient of determination and can be used to predict soil loss from soil excavation surfaces. Meanwhile, the water flow power must reach a certain critical value for soil loss to occur on the slope surface.



(a) Scatter plot



(b) Double-Log plot

Figure 3: Relationship between Darcy-Weisbach resistance coefficient and Reynolds number.

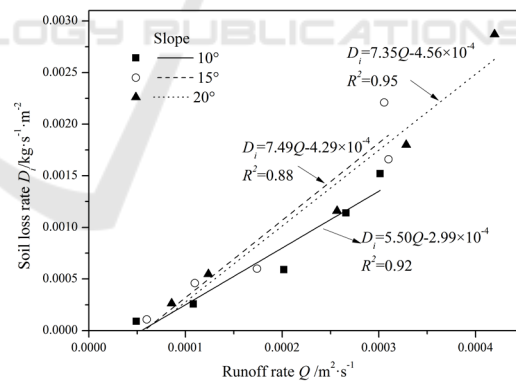


Figure 4: Soil loss rates as functions of runoff rates.

### 3.3 Analysis of Rill Erosion Model on Soil Excavation Slope

Figure 4 shows the relationship between runoff rate and soil denudation rate on the soil excavation slope. Runoff rates of  $4.92 \times 10^{-5}$  to  $3.01 \times 10^{-4} \text{ m}^2\cdot\text{s}^{-1}$  for excavated surfaces with a slope of  $10^\circ$ . When the slope is  $15^\circ$  and  $20^\circ$ , the runoff rate is 0.86 to 1.21 times and 1.14 to 1.74 times, respectively. There was a good linear relationship between soil denudation

rate and runoff rate. Among them, the slopes of the fitted equations were 1.36 and 1.33 times higher for slopes of 15° and 20° than for slopes of 10°, respectively. Therefore, the slope is the key factor affecting soil loss on the slope of soil excavation, and the degree of its influence increases with the slope showing the characteristics of first increasing and then leveling off.

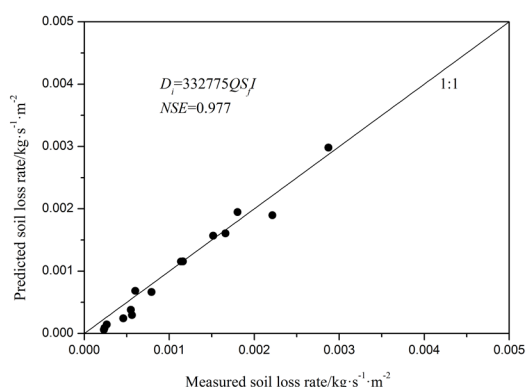
The relationship between soil erosion rates between fine channels on soil excavated slopes and the rainfall runoff factor and topographic factor was obtained by predicting the soil erosion rates between fine channels based on the equations used in the WEPP model for calculating fine channel erosion:

$$(8)$$

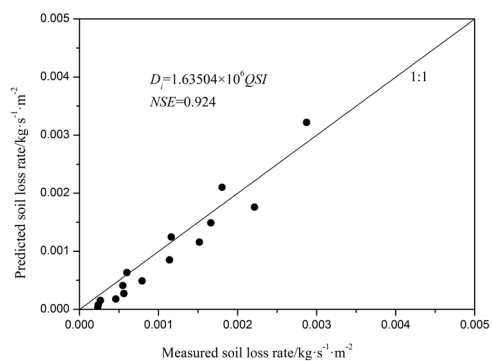
Where,  $D_i$  is the soil erosion rate between rills on the soil excavation slope,  $\text{kg}\cdot\text{s}^{-1}\cdot\text{m}^{-2}$ ;  $Q$  is the average runoff rate of surface runoff,  $\text{m}\cdot\text{s}^{-1}$ ;  $S_f$  is the slope factor;  $I$  is the rain intensity,  $\text{m}\cdot\text{s}^{-1}$ .

The soil erodibility factor  $K_i$  of the soil excavation slope is  $0.332\times 10^6\text{kg}\cdot\text{s}^{-1}\cdot\text{m}^{-2}$  obtained from the regression coefficient of equation (8).

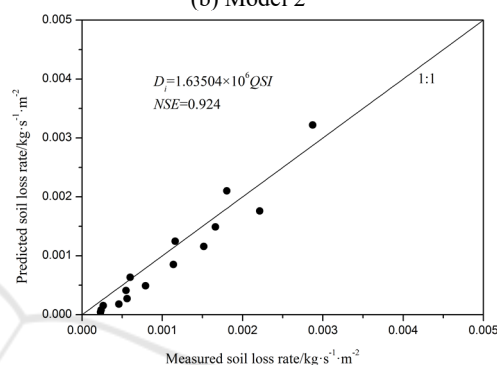
The prediction results of the fine intergully erosion models selected in this study are shown in Figure 5. The Nash efficiency coefficients of model 1, model 2, and model 3 were 0.977, 0.924, and 0.966, respectively, indicating that all three models performed well in predicting soil denudation rates on soil excavation slopes under the rainfall intensity and slope conditions of this study. Model 1 was the best in predicting soil denudation rate on soil excavation slopes. The comparison of the model structures reveals that the calculation results using the convex curve type slope factor index are more accurate.



(a) Model 1



(b) Model 2



(c) Model 3

Figure 5: Comparison between measured and predicted soil losses from the excavated soil slope.

## 4 DISCUSSION

In this paper, the hydrodynamic characteristics of the soil excavation slope are analyzed for its fine interchannel erosion process under rainfall conditions. The soil excavation slope has the characteristics of high compactness, high capacity, low infiltration rate and steep slope, etc. Its process of producing flow and sand is quite different from the natural slope. The erosion mode of the soil excavation slope during the sampling stage of this test is mainly interfine gully erosion, and the hydrological process is mainly surface runoff, which accounts for 67.2~85.4% of the total rainfall. Under the test rainfall conditions, the surface runoff flow pattern on the soil excavated slope with slope of 10°~20° still belongs to laminar flow. However, there is obvious tumbling of fine sand in the test slope surface runoff, which contradicts with the non-mixing of masses between the layers of laminar flow. At the same time, the resistance coefficient of surface runoff from soil excavated slopes is greater than that in open channel laminar flow (Figure 3), and for this phenomenon can be explained from the perspective of slope flow resistance composition. The

slope surface flow resistance includes four components: particle resistance, morphological resistance, wave resistance and rainfall resistance, and these four components can be superimposed on each other. In this study, field rainfall tests were used, with no ground cover on the excavated slope and the slope flow depth  $h$  ranging from 1.04 to 4.03 mm. The median diameter of raindrop is 2.30 mm, because when  $h \leq 3$  mm, the raindrop striking force can penetrate the water layer and affect the topsoil. At the same time, raindrops disturbing the thin layer of water flow on the slope increase the turbulence of the water flow, thus increasing its resistance (Proffitt et al., 1993).

Through the test observation, the erosion process of soil excavation slope surface shows that the thin layer of water flow erosion is dominant, i.e., fine inter-groove erosion. Therefore, the conclusions obtained from this study are applicable to the surface erosion stage of the slope without erosion ditch. Water flow power is suitable for describing the erosion process of thin water flow on slopes, and can reflect the effect of slope water runoff rate and slope factor on soil denudation rate. The sand transport process of slope surface flow caused by rainfall is influenced by the water depth, while the size of the water depth is influenced by the slope. Rain intensity is also an important parameter that influences the erosion process between fine trenches on the slopes of soil excavations (Kinnell, 1988). Through the above analysis, we further added the rain intensity factor into the equation for predicting soil denudation rate. The results show that the prediction accuracy of the model in Table 3 is greater than that of Eq. (7), and the model in Table 3 takes into account the effects of rainfall, runoff and slope on soil denudation rate at the same time. Models 1 and 3 performed better in predicting soil denudation rates compared to model 2, indicating that the convex curve type slope factor index is more suitable for soil denudation rate calculation on soil excavation slopes. The slope of the fitted equation between soil denudation rate and runoff rate under different slope conditions is not a single linear relationship with increasing slope (Figure 4), which is similar to the results of Parson and Abrahams (1993). The amount of erosion between fine trenches showed a tendency to increase and then decrease with increasing surface slope, i.e., there was a critical slope, and this phenomenon was also present on the soil excavation slopes.

Due to the limitation of experimental conditions, only the soil excavation slope was selected for this study to investigate the hydrodynamic characteristics during the erosion between fine trenches. In reality,

there are various forms of engineering excavation slopes, and the composition of the sub-bedding material, the depth of the excavated soil layer and the length of the excavated slope will affect the process of slope hydraulic erosion, and the way of erosion is also diversified, including sheet erosion, fine ditch, shallow ditch and other erosion methods. In this paper, the field excavation surface plot size is small, the material composition of the lower bedding surface is relatively single, the test is not designed separately for different slope lengths, and the erosion process of the excavation slope under the condition of water and sand coming from above is not considered. The later research needs to further study the test plot size, material composition of the lower bedding surface, erosion mode and other aspects, so as to provide reference for the establishment of erosion prediction model for the engineering excavation slope.

Table 3: Efficiency of selected models.

	Equation	NSE
Model 1	$D_r=332775QS^d$	0.977
Model 2	$D_r=1.63504 \times 10^6 QSI$	0.924
Model 3	$D_r=753568QS^{2/3}I$	0.966

## 5 CONCLUSION

By establishing excavated slope plots with different slopes ( $10^\circ$ ,  $15^\circ$  and  $20^\circ$ ) of soil in the field and studying the hydrodynamic characteristics of fine interchannel erosion on excavated slopes under different simulated rainfall intensities (0.6, 1.1, 1.61, 2.12 and 2.54 mm/min) and a design total rainfall of 50 mm, the main conclusions are as follows:

1) The surface runoff from the soil excavation slope is 33.6~42.7 mm, and surface runoff is the main hydrological process, accounting for 67.2~85.4% of the total rainfall. The influence of rainfall intensity on sediment yield is greater than that of slope change.

2) The flow velocity and Reynolds number of the soil excavation surface were highly significantly correlated ( $P < 0.01$ ) with the interaction of rain intensity  $I$  and slope and rain intensity  $I \times S$ . Interaction between Froude number and rain intensity  $I$ , slope  $s$ , slope and rain intensity  $I \times S$  was not related; Manning coefficient, Darcy weisbach resistance coefficient and flow power are not related to rain intensity. There is no obvious relationship between Darcy-Weisbach resistance coefficient and Reynolds number, and the phenomenon of "increasing resistance" exists on the soil excavation slope.

3) All three fine intergully erosion models were able to predict the soil denudation rate of soil excavated slopes better. In terms of fitting effect, model 1 (NSE=0.977) > model 3 (NSE=0.966) > model 2 (NSE=0.924). The convex curve type slope factor index is more suitable for the calculation of soil denudation rate of soil excavation slope. The soil erodibility factor  $K_i$  of the soil excavation slope is  $0.332 \times 10^6 \text{ kg} \cdot \text{s} \cdot \text{m}^{-4}$  calculated from the WEPP inter gully erosion equation (Model 1).

## ACKNOWLEDGMENT

This work is supported by the State Grid Corporation of China (WBS NO.501304200006)

## REFERENCES

- Bulygin, S. Y., Nearing, M. A., & Achasov, A. B. (2002). Parameters of interrill erodibility in the WEPP model. *Eurasian Soil Science C/C of Pochvovedenie*, 35(11), 1237-1242.
- Defersha, M. B., & Melesse, A. M. (2012). Effect of rainfall intensity, slope and antecedent moisture content on sediment concentration and sediment enrichment ratio. *Catena*, 90(3), 47-52.
- Flanagan, D. C., & Nearing, M. A. (1995). *USDA-Water Erosion Prediction Project, hillslope profile and watershed model documentation*. USDA ARS: National Soil Erosion Research Laboratory.
- Kinnell, P. I. A. (1988). The influence of flow discharge on sediment concentrations in raindrop induced flow transport. *Soil Research*, 26(4), 575-582.
- Kinnell, P. I. A. (1993). Runoff as a factor influencing experimentally determined interrill erodibilities. *Soil Research*, 31(3), 333-342.
- Li, G., Abrahams, A. D., & Atkinson, J. F. (2015). Correction factors in the determination of mean velocity of overland flow. *Earth Surface Processes & Landforms*, 21(6), 509-515.
- Luo, R. T., Zhang, G. H., & Cao, Y. (2009). Progress in the research of hydrodynamic characteristics of sediment laden overland flow. *Progress in Geography*, 28(4), 567-574.
- Nearing, M. A., Norton, L. D., & Bulgakov, D. A., Larionov, G. A., West, L. T., & Dontsova, K. M. (1997). Hydraulics and erosion in eroding rills. *Water Resources Research*, 33(4), 865-876.
- Parson, A. J., & Abrahams, A. D. (1993). *Field investigations of sediment removal in interrill overland flow*. UK: UCL Press.
- Proffitt, A. P. B., Rose, C. W., & Lovell, C. J. (1993). Settling velocity characteristics of sediment detached from a soil surface by raindrop impact. *Catena*, 20(1-2), 27-40.
- Pruski, F. F., & Nearing, M. A. (2002). Climate-induced changes in erosion during the 21st century for eight u.s. locations. *Water Resources Research*, 38(12), 34-1-34-11.
- Wang, T. W., Yu, B., Liu, Y. J., & Li, Z. X. (2016). Impacts of road surface shape on soil erosion of rural unpaved road. *Transactions of the Chinese Society of Agricultural Engineering*, 32(19), 162-168.
- Zhang, P. C., Zhou, R., Cheng, D. B., Li, Y. L., & Xu, W. S. (2013). Discussion on characteristics of engineering excavated slope and rapid monitoring technology for soil loss. *Journal of Yangtze River Scientific Research Institute*, 30(9), 24-28.
- Ziadat, F. M., & Taimah, A. Y. (2013). Effect of rainfall intensity, slope and land use and antecedent soil moisture on soil erosion in an arid environment. *Land Degradation and Development*, 24(6), 582-590.